

Article

Analysis of Waste Tire Particle Movement in a Single Horizontal-Axis Stirred Reactor Based on the Eulerian Discrete Element Method

Litong Hou ¹, Yicheng Wu ¹, Xiaomin Chen ², Junrong Liu ² and Yongzhi Ma ^{1,*}

¹ College of Mechanical and Electrical Engineering, Qingdao University, Qingdao 266071, China; hlt@qdu.edu.cn (L.H.)

² Qingdao Wanfang Recycling Technology Co., Ltd., Qingdao 266071, China

* Correspondence: qdhiking@qdu.edu.cn

Abstract: The pyrolysis of waste tires has been considered a potential sustainable solution in light of escalating carbon dioxide emissions. Nevertheless, current research indicates a lack of comprehensive understanding regarding the movement of waste tire particles in a single horizontal-axis stirred pyrolysis reactor. This study employed EDEM 2021.2 software to perform comprehensive numerical simulations of a single horizontal-axis stirred pyrolysis reactor, examining the impact of three main production factors—particle size, feed rate, and central axis speed—on particle motion. By acquiring contact data between particles and reactor walls, we illustrated the persistent motion of particles during the operation of the equipment. The research findings suggest that with the rise in rotational speed, there is a corresponding increase in particle accumulation. In high-speed conditions, the interaction between particles and the reactor wall is intensified. The contact level increased by 15.54% (at 3 r/min) and 25.66% (at 5 r/min) with the rise in rotational speed. Furthermore, at an identical rotational speed, the interaction between the larger particle group and the wall surpassed that of the smaller particle group. Doubling the feed rate led to a reduction of over 10% in the contact level between particles and the reaction wall at varying speeds. Through a thorough analysis of various factors influencing particle motion, our objective is to elucidate the motion traits of particles in the reactor, offering crucial theoretical direction and technical assistance to enhance production efficiency and ensure the secure and steady operation of pyrolysis reactors.

Keywords: recycling; tire particles; pyrolysis; single horizontal-axis stirred reactor; particle motion; discrete element method; EDEM



Citation: Hou, L.; Wu, Y.; Chen, X.; Liu, J.; Ma, Y. Analysis of Waste Tire Particle Movement in a Single Horizontal-Axis Stirred Reactor Based on the Eulerian Discrete Element Method. *Sustainability* **2024**, *16*, 2301. <https://doi.org/10.3390/su16062301>

Academic Editors: Harshit Mahandra, Farzaneh Sadri and Monu Malik

Received: 17 February 2024

Revised: 4 March 2024

Accepted: 6 March 2024

Published: 11 March 2024



Copyright: © 2024 by the authors. Licensee MDPI, Basel, Switzerland. This article is an open access article distributed under the terms and conditions of the Creative Commons Attribution (CC BY) license (<https://creativecommons.org/licenses/by/4.0/>).

1. Introduction

The automotive industry is one of the driving forces behind global industrial development. With the growth of global and automotive industries, there has been an increasing demand for automobiles. Consequently, the production of waste tires has escalated. The proper disposal and recycling of waste tires has become a pressing social issue [1,2]. Improper handling of waste tires can pose significant threats to the environment and human health [3,4] and also disrupt the ecological balance. Hence, implementing rational waste tire management and recycling is crucial to protect the environment and conserve resources. Only through responsible utilization and treatment of waste tires can their adverse impacts on the environment and human health be mitigated while contributing to a circular economy and sustainable development [5]. Owing to their poor biodegradability in the environment [6], safe disposal and recycling measures are imperative.

Pyrolysis has gained significant attention as the most effective and thorough method of tire disposal and is a promising recycling approach [7–9]. Pyrolysis allows for the recovery of energy and valuable gas, liquid, and solid fractions from scrap tires [10]. However, the efficiency of the process largely depends on the type of cracking reactor [11]. Waste tire

cracking equipment can be categorized into various types [12]. Ünsaç et al. [13] studied the efficiency of screw mixing and conveying, as well as the performance of the reactor, heating gas pipeline, and cyclone separator using a rotating batch reactor and an improved belt screw conveyor. The improved strip screw design increased the level of technical preparation. Choi et al. [14] comprehensively analyzed the product yield and properties of the fluidized bed system and compared it with the fixed bed system. The potential use of fluidized bed reactor for pyrolysis was evaluated to overcome the main limitations of the traditional pyrolysis process. Qi et al. [15] used a pilot-scale spiral propulsion reactor to study the pyrolysis characteristics of waste truck tires (WT1) and waste passenger car tires (WT2). The results showed that at four pyrolysis temperatures, the solid yield of WT2 was higher than that of WT1, and the liquid and gas yield were lower than that of WT1. Wang et al. [16] investigated the impact of temperature and pressure on product distribution in catalytic slow pyrolysis in a fixed bed and catalytic fast pyrolysis in a fixed fluidized bed. The use of a catalyst enhanced styrene yield and decreased secondary reaction occurrence. Wang et al. [17] studied the effect of flue gas on waste heat transfer and reaction by establishing a numerical simulation model. The results show that the temperature distribution and particle size change of different components, as well as the influence of flue gas temperature and velocity, have an impact on the pyrolysis process.

The software EDEM, short for Eulerian discrete element method, was developed for bulk material simulation. Its primary functions involve simulating the dynamic behavior of particle systems and coupling physical processes like particle–fluid interactions, particle structure, and heat conduction, aiding users in understanding and predicting particle system behavior. The software finds wide application in mining, metallurgy, energy, pharmaceuticals, and food-processing industries. Additionally, EDEM offers an intuitive visual interface and robust post-processing tools. Users can assist and guide engineering applications by analyzing simulation results, generating reports, and optimizing designs. It aids engineers and researchers in process optimization and equipment design enhancement. Liu et al. [18] used the discretization method to simplify the problem and calculate higher accuracy. Monfared et al. [19] used the discrete element method to simulate the behavior of packed granular beds, focusing on the generation of densely packed granular beds. The optimal rolling friction coefficient is proposed to accurately represent the dense spherical carbon particle bed. Hilse et al. [20] used the discrete element method (DEM) to numerically analyze the intermittent single-layer contact heat transfer of a multi-bottom furnace. The average heat loss parameters were determined. The results show that the blade angle has little effect on the time evolution of particle temperature, but the frequency distribution is affected by the blade angle, and the standard deviation increases with the increase in the angle of the blade. Liu et al. [21] proposed an experimental method to determine the sliding friction coefficient between different particles and boundaries and embedded the results into DEM software for verification. This method was found to improve the accuracy of the DEM simulation results. Cleary et al. [22] Applied the fully bidirectional coupled particle size model based on DEM and SPHS methods to the SAG mill. Scale up the model of industrial scale equipment. Chen et al. [23] in this study, a CFD-DEM coupling modeling method based on soft sphere and porous model was proposed to explore the material transfer mechanism of gas liquid solid mixed flow. It provides theoretical reference and technical support for the material conveying mechanism and production process.

Proch et al. [24] found that the length of a rotary kiln increased with an increase in the bed particle mass flow while the inclination angle and rotational speed remained constant. Hu et al. [25] proposed a two-stage rotary kiln reactor with baffles to enhance the flowability of material particles in the dead zone. The study of particle movement and mixing inside the reactor lays the foundation for subsequent device debugging and process parameter settings [26]. Liu et al. [27] found through numerical simulations that the mixing effect at higher speeds was significantly better than that at lower speeds in a twin-screw pyrolysis reactor. Xie et al. [28] found that the heating rate significantly increased with an increase in the rotary drum reactor speed. Kwapinska et al. [29] studied the motion of particles in

a horizontal rotary drum and indicated the advantages of the discrete element model in simulating particle behavior. Navarro et al. [30] analyzed the effect of different process conditions on the solid particles of different materials and found that particle size had the greatest influence. Zheng et al. [31] conducted thermal simulations with different particle sizes and rotational speeds inside a rotary kiln, revealing that increasing the rotational speed ensured a uniform temperature increase and a smaller particle size improved the heat transfer effect. A smaller tire particle size increases the surface area of the particles, indicating a larger heat-exchange surface. A smaller tire particle size also shortens the heat-diffusion path. According to Fourier's law for heat transfer, smaller tire particle sizes can improve the heat transfer efficiency. According to the relevant literature, when the tire particle size is small, the heat transfer barrier layer is also smaller, and the tire sample can quickly receive heat, allowing the temperature of the waste tire particles to rise rapidly [32]. Zhang et al. [33], in their study of individual particles, observed that the uniformity of particle temperature initially decreased and then increased with a decrease in filling rate. Han et al. [34] improved the heat transfer efficiency between the reactor and the particles by adding a heat carrier within the reactor.

Previously, a fixed filling rate or reduced model was mostly used to analyze the motion characteristics of particles in equipment. Nevertheless, without an actual model and data on feeding and discharging states during production, this method fails to fully depict the motion characteristics of particles in real work conditions. In this research, the discrete element method is employed to simulate the impact of three key production factors on particle dynamics in the reactor: particle size, feed rate, and central shaft speed. Using this approach allows for a more precise insight into particle motion under real operating conditions, offering enhanced references and guidance for optimizing the production process.

2. Physical Model and Theoretical Model

2.1. Physical Model and Actual Equipment

This study presents the structural diagram of a single horizontal-axis stirred pyrolysis reactor in Figure 1. The reactor consists mainly of a pyrolysis furnace tube, a central shaft, stirring arms, stirring teeth, a support structure, and other fundamental components. These components collaborate to facilitate the stable movement of waste tire particles within the reactor. The actual photograph of the reactor in operation is depicted in Figure 1b and was provided by China Qingdao Wanfang Recycling Technology Co., Ltd. (Qingdao, China).

During the design, in order to ensure the stability and reliability of equipment operation, a support structure is set in the middle of the central axis to improve its stiffness and prevent deformation and vibration. The central shaft is connected with the mixing teeth through the mixing arm. The mixing arm is evenly distributed on the central shaft, arranged at a certain angle, and the end is connected with the mixing teeth. The central shaft is driven by an external motor. Driven by the central shaft, the mixing teeth rotate at the same angular speed.

During the normal operation of the single horizontal shaft stirred pyrolysis reactor, the particles move under the drive of the stirring teeth, collide and slide in the movement, and exchange positions, and the temperature gradually increases during the heating process. Finally, thermal decomposition occurs, forming a series of pyrolysis products such as carbon black, steel wire, pyrolysis gas, and pyrolysis oil. The carbon black moves with the movement of the stirring teeth and finally enters the tail of the pyrolysis reactor for gravity collection in the carbon black collection device. This design makes the continuous feeding and pyrolysis of waste tire particles possible, which is in line with the objectives of environmental protection and resource recovery.

This design has a simple and stable operation, is not prone to coking, and solves the common coking problem in pyrolysis reactors, greatly improving the stability of reactor operation. This device is suitable for various types of waste tire recycling and has significant practical value.

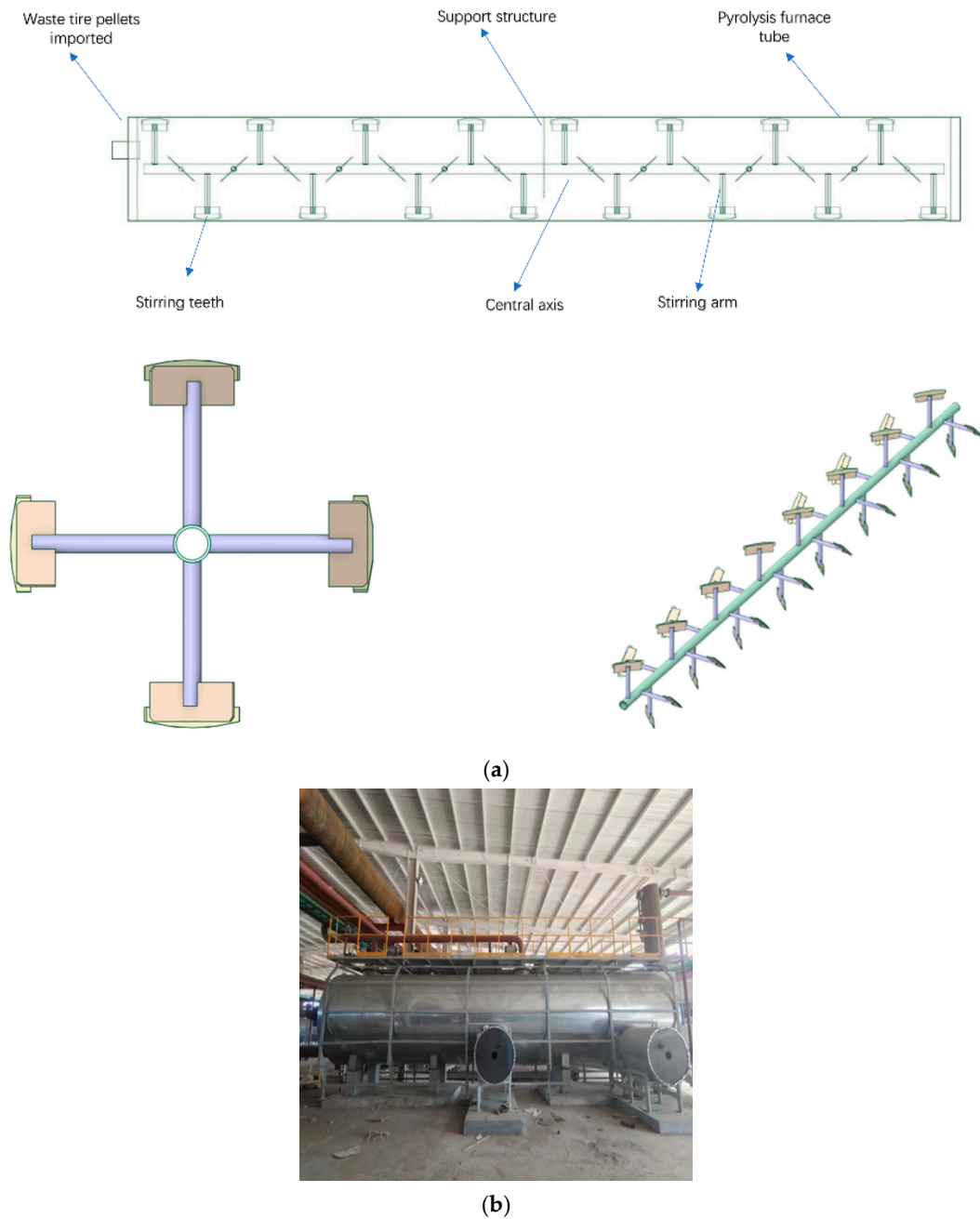


Figure 1. (a) Equipment model and (b) physical diagrams of a single horizontal-axis stirred pyrolysis reactor.

2.2. Theoretical Model

By applying the Hertz–Mindlin (nonslip) contact model and the standard rolling friction theory model in the discrete element method, we assume that the structural parameters and physical significance of the former involve setting the radii of the two spherical particles to R_1 and R_2 . When elastic contact occurs between these particles, the calculation formula for the normal overlap amount, δ_n (Equation (1)), is used.

$$\delta_n = R_1 + R_2 - |r_1 - r_2| \quad (1)$$

In the formula above, r_1 , r_2 are the position vectors of two pellet centers.

The normal force between the two particles, F_n , is calculated as shown in Equation (2).

$$F_n = \frac{4}{3} E^* \sqrt{R^*} d_n^{1.5} \quad (2)$$

In the formula above, E^* and R^* are the equivalent tensile modulus of elasticity and equivalent radius of particles, respectively.

E^* , R^* are shown in Equations (3) and (4), respectively.

$$\frac{1}{E^*} = \frac{1 - v_1^2}{E_1} + \frac{1 - v_2^2}{E_2} \quad (3)$$

$$\frac{1}{R^*} = \frac{1}{R_1} + \frac{1}{R_2} \quad (4)$$

In the formulas above, E_1 , v_1 , and E_2 , v_2 are the tensile moduli of elasticity and Poisson's ratios of particles 1 and 2, respectively. The normal damping force, F_n^d , is expressed as shown in Equation (5).

$$F_n^d = -2\sqrt{\frac{5}{6}}\beta\sqrt{S_n m^* v_{n-rel}} \quad (5)$$

In the formula above, β is the coefficient; S_n is the normal stiffness; m^* is the equivalent mass; and v_{n-rel} is normal component of relative velocity.

The mathematical expression for β as shown in Equation (6) is

$$\beta = \frac{\ln a}{\sqrt{\ln^2 a + \pi^2}} \quad (6)$$

In the formula above, a is the coefficient of restitution.

To objectively describe the influence of different factors on the contact effect between particles and walls, the contact degree is defined as ψ using Equation (7), where N is the number of particles in contact with the reactor wall, and M is the total number of particles in the reactor.

$$\psi = \frac{N}{M} \quad (7)$$

2.3. Computation Model

The fundamental assumption of the discrete element method is to treat each particle as an independent entity, where the entire particle system consists of a collection of discrete particles. To facilitate theoretical analysis, the following assumptions are made in this study:

1. Assumption of rigid particles: In this study, the particles were assumed to be rigid, implying that the shape of the spherical particles did not change when they collided. This assumption helps simplify the model and reduces computational complexity.

2. Point contact model: This study considers a point contact model, assuming that contact between particles occurs at discrete points rather than over the entire contact area. This assumption simplifies the contact model, reduces computational effort, and is suitable for modeling the interaction forces between particles.

3. Soft-sphere model: A soft-sphere model was employed in this study as the contact model. This implies that the contact between the particles possesses a certain degree of softness, allowing for the formation of cohesive forces and considering the elastic deformation of the particles during the contact process.

These assumptions in the discrete particle numerical simulation serve as a foundation for modeling the behavior of particle systems during waste tire pyrolysis. They provide a basis for understanding the particle interactions, contact forces, and overall dynamics of the system, contributing to the optimization and design of waste tire pyrolysis equipment.

To simplify the calculation and simulation processes, waste tire particles were defined as spherical particles in this study, and their parameters are listed in Table 1. In the actual pyrolysis process, the shape and size of waste tire particles may change from angular to elliptical. However, by defining a particle as a sphere, the simulation process can be simplified to a certain extent, and an effective method is provided to study the motion behavior of the particles. These assumptions are suitable for simulating the movement of tire particles in a moving-bed reactor. Relevant studies were conducted to simulate the

particle size after simplification, and relevant experiments were performed on the residence time of the particle group with a change in the rotating speed [35]. The comparison results show that the experimental results are in good agreement with the simulation results, which are consistent with the actual operational results of the equipment. It can be concluded that the movement time of the particles after simplification agrees with the actual operation, and the surface simplification does not affect the study of particle movement.

Table 1. Particle coefficient. Material property settings reference [35].

Parameter	Code	Value
Particle generation rate	M	0.16 kg/s
Particle radius	r	10 mm
Particle Absorption Rate	$\epsilon\sigma$	0.875
Particle density	ρ	1020 kg/m ³
Specific heat capacity of particles	C_p	1300 J/(kg·K)
Recovery factor		
Pellets/Pellets	e_{pp}	0.421
Particle/wall surface	e_{pw}	0.313
Static friction coefficient		
Pellets/Pellets	f_{pp}	0.7
Particle/wall surface	f_{pw}	0.5
Rolling friction coefficient		
Pellets/Pellets	f'_{pp}	0.5
Particle/wall surface	f'_{pw}	0.3
Time step	Δt	1.6×10^{-4} s
Data saving interval	Δt_s	0.01 s

By defining the waste tire particles as spherical, the classical discrete particle numerical simulation method can be used for simulations and calculations. By setting different particle radii (7.5, 10, and 15 mm), central shaft speeds (1, 3, and 5 r/min), and feed speeds (0.16 kg/s and 0.32 kg/s) at the feed inlet, the movement process of particles in the reactor under different factors and the influence of various factors on particle movement were explored.

When using the EDEM software to simulate the feeding process of equipment, it is necessary to create particles and define their physical properties. Subsequently, a particle factory plane was created in the scene and set as a virtual face. We used this virtual face as the particle-generation face and set its position, size, shape, and generation speed. Simultaneously, we also needed to set appropriate physical conditions for the boundary. Ultimately, the particle-generation mode was set. For equipment design, a rectangular opening was set at the end of the equipment. When the particles moved to this point, they were affected by gravity, fell from the opening, and left the model. Through the steps above, the equipment feeding and discharging processes can be accurately simulated and analyzed.

During the pyrolysis of waste tire particles, the reactor is typically kept fully closed to prevent leakage of the gas product. Therefore, this study focuses on the movement characteristics of waste tire particles in a reactor during pyrolysis. The discrete element method (DEM) via simulation software EDEM was used to visualize the movement of waste tire particles under different conditions, such as rotating speed, particle size, and feeding speed. The influence of these factors on particle motion behavior was analyzed in detail. These studies help reveal the movement characteristics of waste tire particles in the reactor and provide important theoretical guidance and technical support for improving the production efficiency and ensuring the safe and stable operation of the pyrolysis reactor.

3. Result Analysis

3.1. Particle Movement at Different Speeds

As shown in Figure 2, when the rotation speed of the central shaft was low, particles accumulated at the feed inlet, resulting in an increase in the height of particle accumulation

during axial conveying. This accumulation is not conducive to contact between the particles and the wall. With an increase in the rotation speed, the height of particle accumulation gradually decreased. With an increase in the rotating speed, the particles can move to a higher position in the vertical direction to improve the contact effect between the particles and the wall. When the velocity is high, it can not only reduce the accumulation of particles at the feed port but also improve the accumulation state of particles in a short time, making it easier for them to contact the wall.

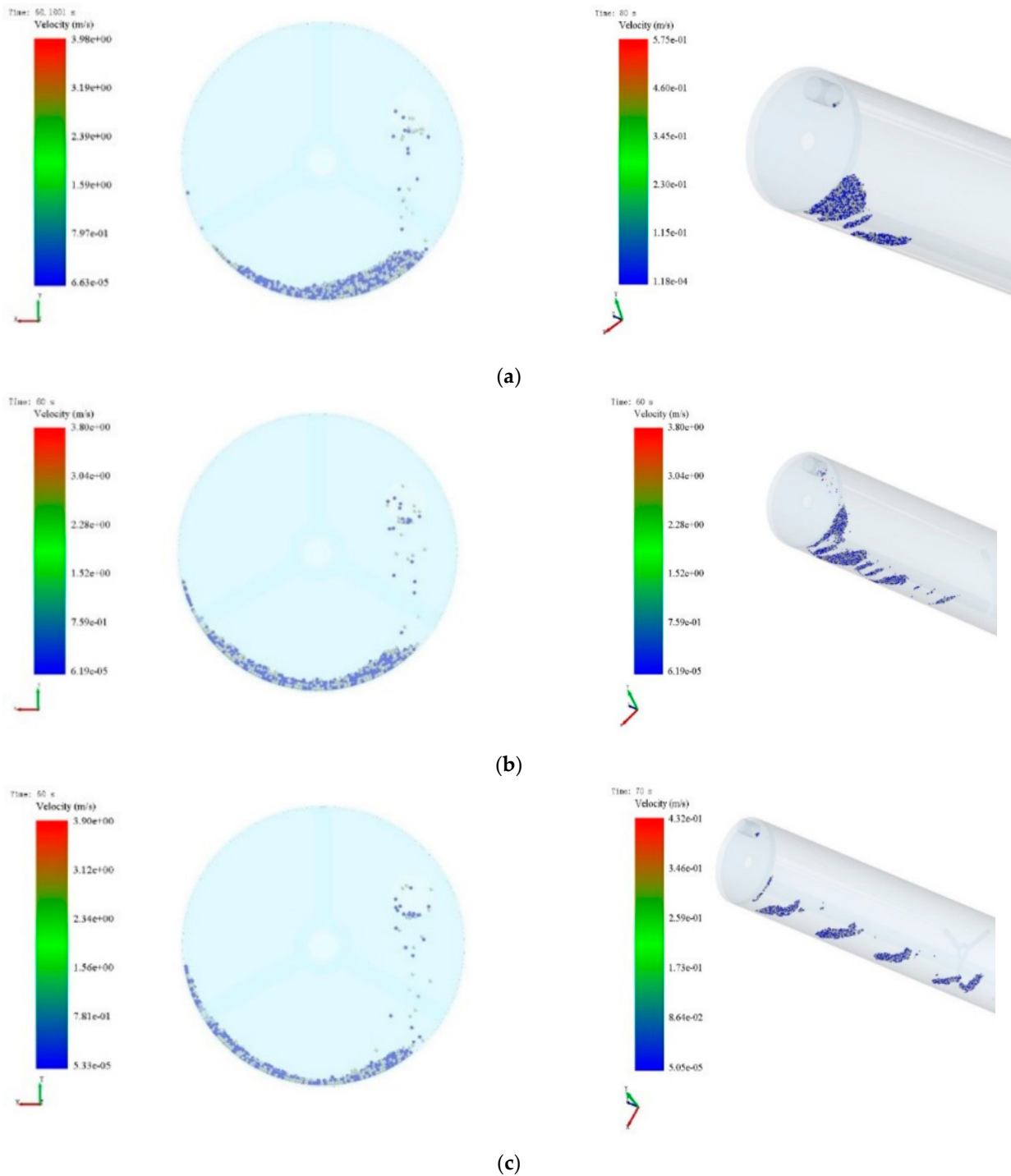


Figure 2. Schematic diagram of 10 mm rigid particle movement at different speeds: (a) 1 r/min; (b) 3 r/min; (c) 5 r/min.

As depicted in Figure 3, an increase in the rotational speed of the central axis leads to a higher contact degree value, enhancing the interaction between particles and the wall. More effective contact between particles and the wall facilitates heat transfer from the particles to the wall. At low speeds, inadequate velocity causes particles to accumulate at the feeding port during continuous feeding, hindering the rapid enhancement of their accumulation state and reducing contact between particles and the wall.

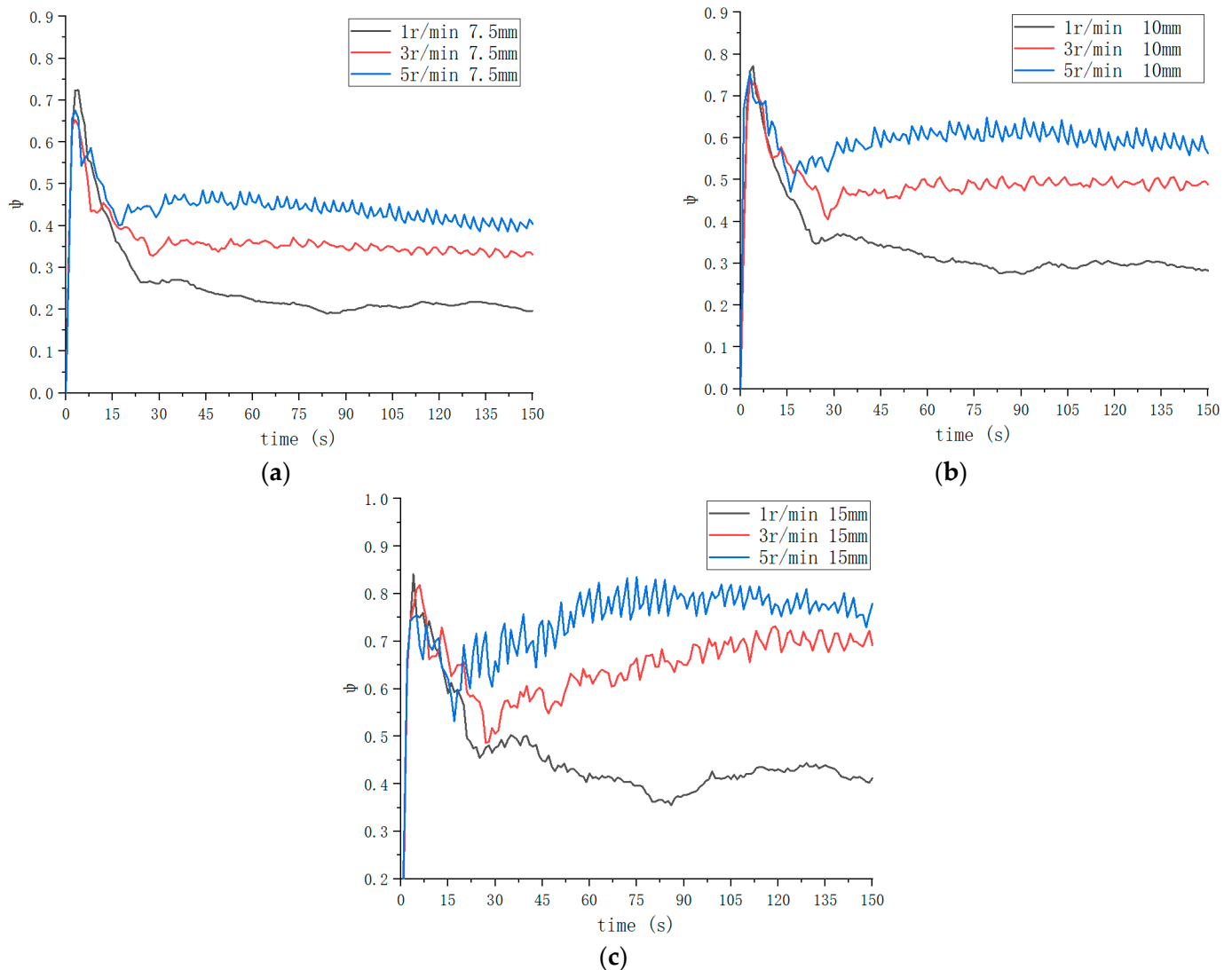


Figure 3. The range of contact degree at different speeds: (a) 7.5 mm; (b) 10 mm; (c) 15 mm.

As shown in Figure 3b, taking the 10 mm particle size as an example, the average contact degree is 0.34 when the speed is 1 r/min. When the speed is 3 r/min, the average value of contact is 0.50. When the speed is 5 r/min, the average contact degree is 0.6. From the data above, it can be seen that as the central shaft speed increases, the average contact degree will also increase accordingly.

3.2. Different Filling Rates

As shown in Figures 2 and 4, with an increase in the feeding speed, the agitator could not handle the particles at the feed inlet in time, resulting in their accumulation at the reactor feed inlet. With time, even if the central shaft has a higher speed, the problem of particle stacking cannot be solved quickly. Compared with 0.16 kg/s, at the same speed and position, the faster the feeding speed, the greater the possibility of particle accumulation.

The accumulation of particles may also cause local temperature changes, which increase the heat transfer resistance of the area where the particles accumulate.

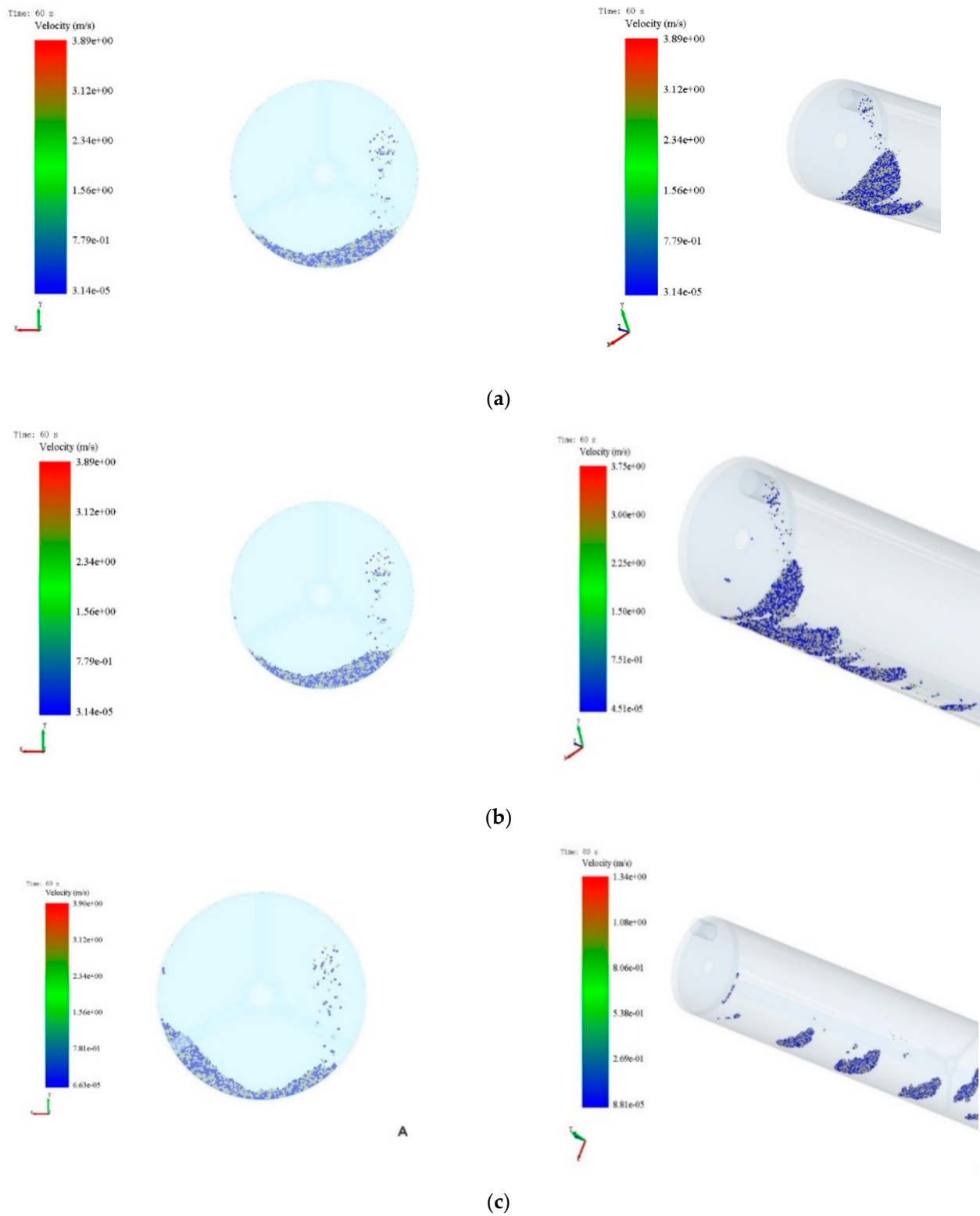


Figure 4. Schematic diagram of the movement of 10mm particles with higher filling rates at different rotational speeds: (a) 1 r/min; (b) 3 r/min; (c) 5 r/min.

Figure 5 shows a schematic diagram of the contact degree comparison under different feed rates. After analyzing the contact degree at different feed rates, it was found that

the average difference in contact degree was 0.1 when the speed was 1 r/min. At a speed of 3 r/min, the average difference between the two is 0.13. When the speed is 5 r/min, the average difference between the two values is 0.15. It can be concluded that when the feed rate doubles, the average contact degree decreases by at least 10%, and as the speed increases, the difference between the average values of the two increases.

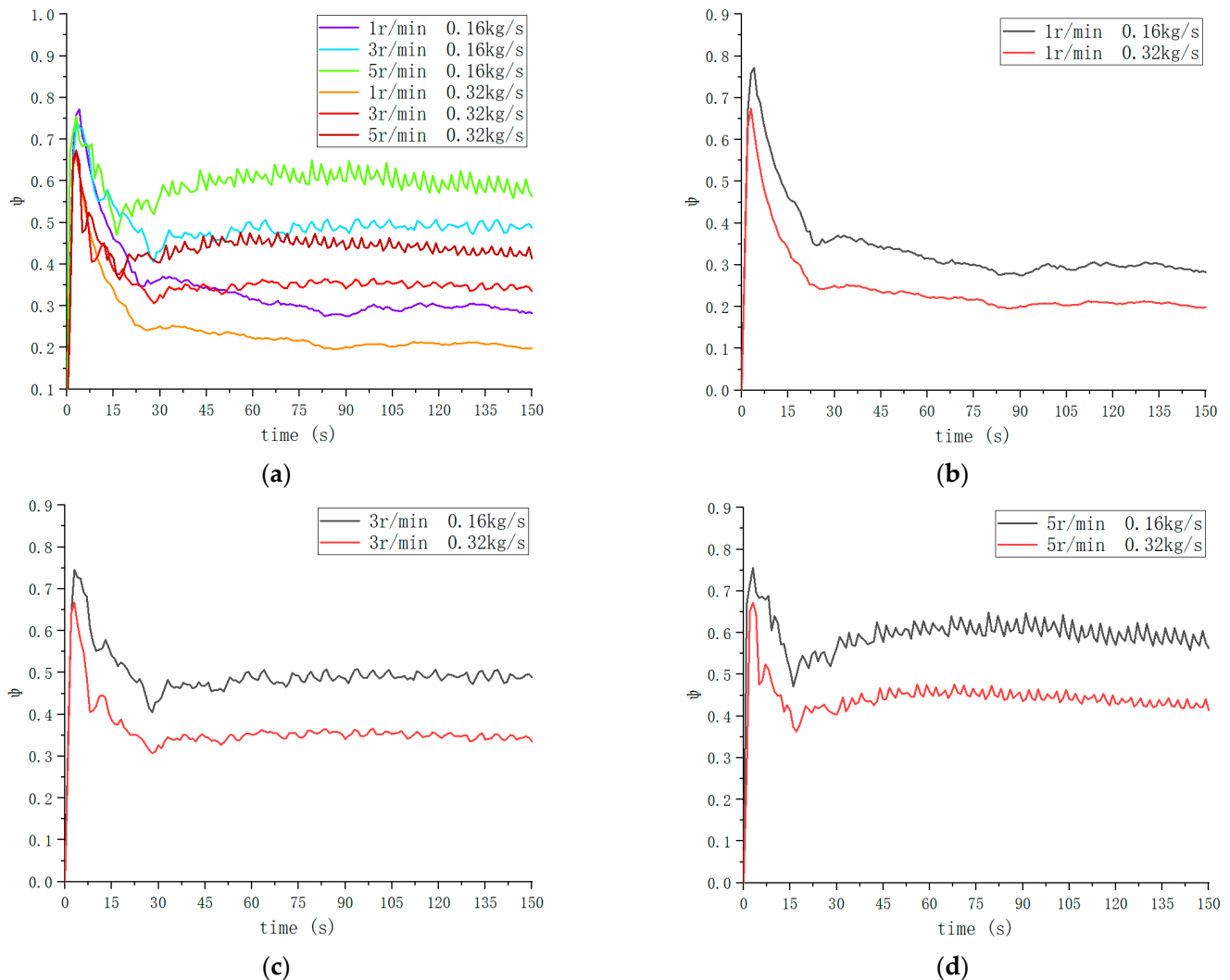


Figure 5. Schematic diagram of contact degree comparison at different feed rates: (a) overview map; (b) 1 r/min; (c) 3 r/min; (d) 5 r/min.

3.3. Particles with Different Particle Sizes

Upon entering the reactor, particles move forward propelled by the stirring teeth, as depicted in the comparison of Figures 2 and 6. Additionally, the 15 mm particles display comparable axial movement to the 7.5 mm and 10 mm particles due to friction against the reactor wall [36]. When central axis velocities are low, particles gather at the inlet; yet limited particle numbers result in a relatively low accumulation height. With increased speed, the stacking height of 15 mm waste tire particles at the inlet decreases, leading to a reduced duration of the stacking process. Consequently, particles can efficiently contact the reactor wall surface upon entry, facilitating effective heat transfer.

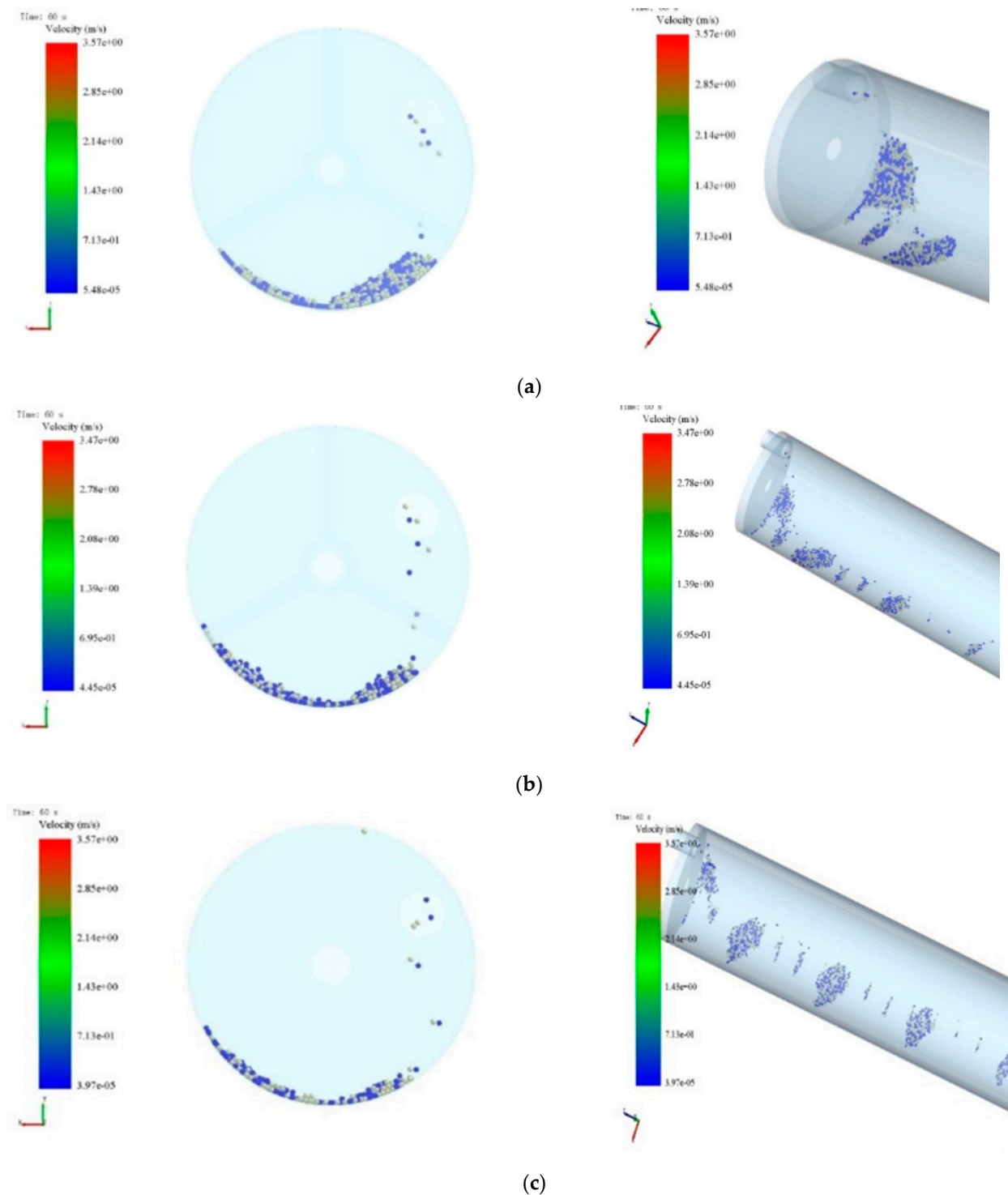


Figure 6. Schematic diagram of 15 mm particle movement: (a) 1 r/min; (b) 3 r/min; (c) 5 r/min.

As shown in Figure 7, among the three types of particles with particle radii of 7.5 mm, 10 mm, and 15 mm, the larger particle exhibits a higher degree of contact. The average contact degree of the 15 mm particles is 10% higher than that of the 10 mm particles. The average contact degree of the 15 mm particles is 20% higher than that of the 7.5 mm particles. This implies that, under identical conditions, an increase in particle size results in enhanced contact, with the value discrepancy in contact growing as the size difference between particles increases.

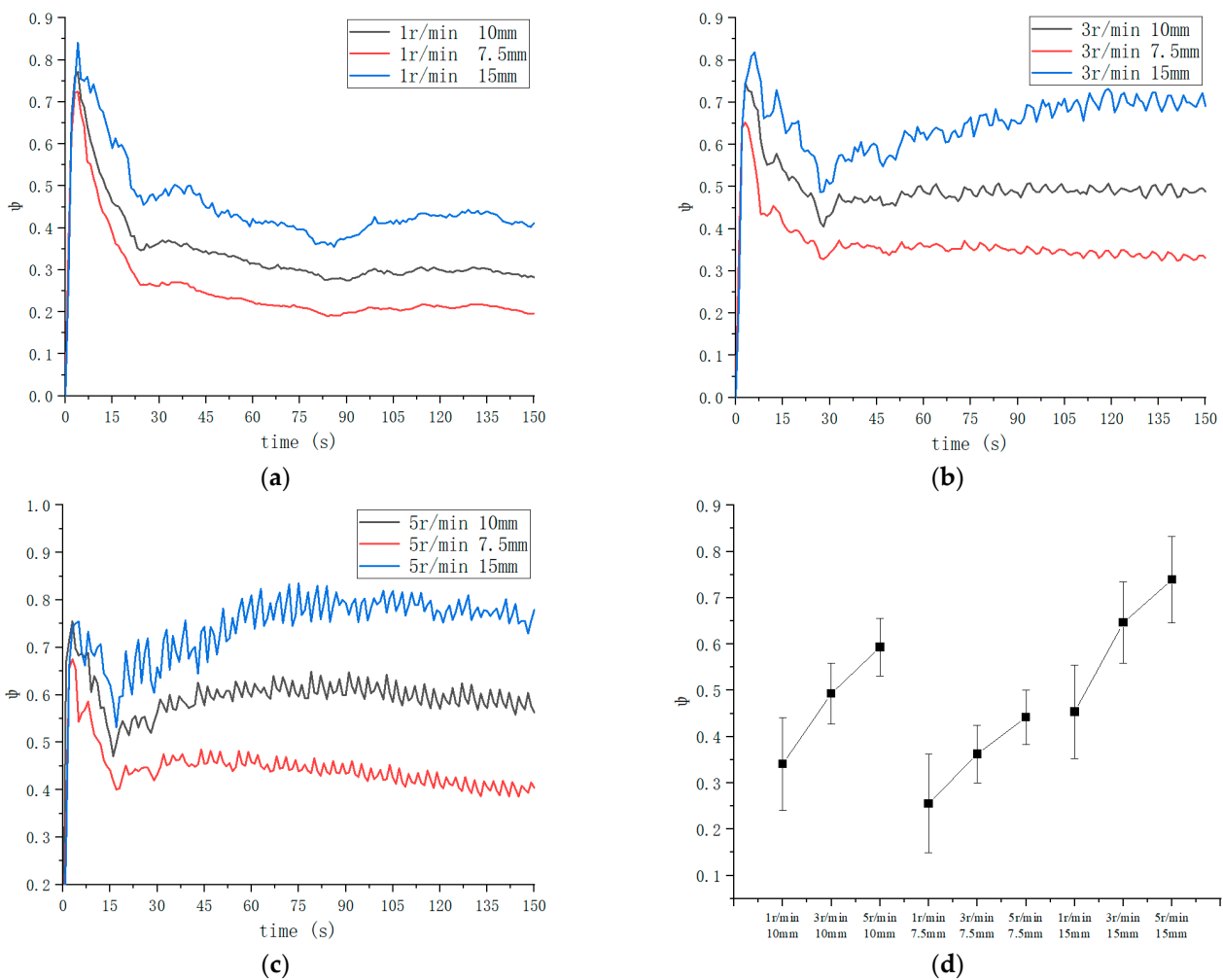


Figure 7. Contact degree distribution and error bars of different particle sizes: (a) 1 r/min; (b) 3 r/min; (c) 5 r/min. (d) Error bar chart.

4. Conclusions

A three-dimensional model of a single horizontal shaft-stirred reactor was established to simulate the effects of three actual production factors on the movement of particles in the reactor: particle size, feed rate, and central shaft speed. The main conclusions are as follows.

(1) With an increase in the central axis speed, the degree of contact between the particles and reactor wall increased, and the contact effect between the particles and reactor wall was optimal when the central axis speed was 5 r/min. At the same rotating speed, with an increase in particle size, the contact effect between the particles and the wall improved, and the particle size had a significant impact on the degree of contact. When the feed rate was 0.32 kg/s, the particles accumulated obviously at the feed inlet, which was not conducive to the contact between the particles and the reactor wall.

(2) Under the actual working conditions of a single horizontal shaft-stirred reactor, the particles moved continuously under the action of the stirring teeth, which realized the design requirements of the continuous operation of the reactor, in which the particles moved axially along the central axis. Simultaneously, the accumulation state of the particles is also improved during the movement process. A higher rotating speed, larger particle size, and smaller feed rate can improve particle accumulation, which improves the contact effect between the particle group and the reactor wall.

(3) Visualization research using the discrete element method simulation software EDEM was helpful in revealing the movement characteristics of particles in the reactor

and verifying the reliability of continuous operation of the reactor and the influence of various factors on the movement of internal particles. This provided important theoretical guidance and technical support to ensure the safe and stable operation of the pyrolysis reactor. Owing to the actual conditions, it was impossible to conduct an actual cold-state experiment, and such an experiment should be performed in the future when the conditions permit. In future research, further theoretical support can be provided for the improvement and operation of equipment by exploring two heat transfer methods, including radiation and heat conduction, for particles inside the reactor through the secondary development of software.

Author Contributions: Conception and research design: L.H.; Article check: Y.M. and Y.W.; Data analysis: L.H.; Provision of the model: J.L. and X.C.; Paper writing: L.H. All authors have read and agreed to the published version of the manuscript.

Funding: This research was funded by National Natural Science Foundation of China (Grant No. 51575286), Key R&D plan of Shandong Province (public welfare science and technology research) (Grant No. 2018GGX 105007).

Data Availability Statement: Data are contained within the article.

Conflicts of Interest: Authors Xiaomin Chen and Junrong Liu were employed by the company Qingdao Wanfang Recycling Technology Co., Ltd. The remaining authors declare that the research was conducted in the absence of any commercial or financial relationships that could be construed as a potential conflict of interest.

References

- Hwang, J.G.; Lee, B.K.; Choi, M.K.; Park, H.C.; Choi, H.S. Optimal Production of Waste Tire Pyrolysis Oil and Recovery of High Value-Added D-Limonene in a Conical Spouted Bed Reactor. *Energy* **2023**, *262*, 125519. [CrossRef]
- Ma, Q.; Mao, Z.; Lei, M.; Zhang, J.; Luo, Z.; Li, S.; Du, G.; Li, Y. Experimental Investigation of Concrete Prepared with Waste Rubber and Waste Glass. *Ceram. Int.* **2023**, *49*, 16951–16970. [CrossRef]
- Campos, A.L.; Lara, L.M.; Ramirez, M.L.C.; Gonzalez, Y.A.L.; Rodriguez, L.B.R.; Moreno, R.D.P.; Sotelo, M.T.F.; Fleites, G.L.; Solar, L.A.P.; Zepeda, J.S.H. Acute and Chronic Toxicity of Waste Tire Ash in *Daphnia Magna*. *Appl. Ecol. Environ. Res.* **2022**, *21*, 713–723. [CrossRef]
- Swilam, A.; Tahwia, A.M.; Youssf, O. Effect of Rubber Heat Treatment on Rubberized-Concrete Mechanical Performance. *J. Compos. Sci.* **2022**, *6*, 290. [CrossRef]
- Kouhi, F.; Vahidifar, A.; Naderi, G.; Esmizadeh, E. Tire-Derived Reclaimed Rubber as a Secondary Raw Material for Rubber Foams: In the Framework of Circular Economy Strategy. *J. Polym. Res.* **2023**, *30*, 97. [CrossRef]
- Mustata, F.S.C.; Asandulesa, M.; Varganici, C.-D.; Curteza, A. Composites Based on Cotton Fabrics, Acrylic Rubber and Powder from Used Tires: Thermal and Electrical Characterization. *J. Therm. Anal. Calorim.* **2023**, *148*, 3325–3339. [CrossRef]
- Han, W.; Han, D.; Chen, H. Pyrolysis of Waste Tires: A Review. *Polymers* **2023**, *15*, 1604. [CrossRef]
- Paul, S.; Rahaman, M.; Ghosh, S.K.; Katheria, A.; Das, T.K.; Patel, S.; Das, N.C. Recycling of Waste Tire by Pyrolysis to Recover Carbon Black: An Alternative Reinforcing Filler. *J. Mater. Cycles Waste Manag.* **2023**, *25*, 1470–1481. [CrossRef]
- Tsipa, P.C.; Phiri, M.M.; Iwarere, S.A.; Mkhize, N.M.; Phiri, M.J.; Hlangothi, S.P. The Effect of Pre-Pyrolysis Chemical Treatment of Waste Tyre Rubber Crumbs: Comparison between Pre-Treated and Conventional Waste Tyre-Derived Oil. *J. Chem. Technol. Biotechnol.* **2023**, *98*, 1279–1289. [CrossRef]
- Costa, S.M.R.; Fowler, D.; Carreira, G.A.; Portugal, I.; Silva, C.M. Production and Upgrading of Recovered Carbon Black from the Pyrolysis of End-of-Life Tires. *Materials* **2022**, *15*, 2030. [CrossRef]
- Roy, C.; Darmstadt, H.; Benallal, B.; Amen-Chen, C. Characterization of Naphtha and Carbon Black Obtained by Vacuum Pyrolysis of Polyisoprene Rubber. *Fuel Process. Technol.* **1997**, *50*, 87–103. [CrossRef]
- Benallal, B.; Roy, C.; Pakdel, H.; Chabot, S.; Poirier, M.A. Characterization of Pyrolytic Light Naphtha from Vacuum Pyrolysis of Used Tyres Comparison with Petroleum Naphtha. *Fuel* **1995**, *74*, 1589–1594. [CrossRef]
- Low Tar Yield and High Energy Conversion Efficiency in a Continuous Pyrolysis Reactor with Modified Ribbon Screw Conveyor—ScienceDirect. Available online: <https://www.sciencedirect.com/science/article/pii/S0360319923062006> (accessed on 3 March 2024).
- Choi, Y.; Wang, S.; Yoon, Y.M.; Jang, J.J.; Kim, D.; Ryu, H.-J.; Lee, D.; Won, Y.; Nam, H.; Hwang, B. Sustainable Strategy for Converting Plastic Waste into Energy over Pyrolysis: A Comparative Study of Fluidized-Bed and Fixed-Bed Reactors. *Energy* **2024**, *286*, 129564. [CrossRef]
- Qi, J.; Hu, M.; Xu, P.; Zhu, F.; Yuan, H.; Wang, Y.; Chen, Y. Study on Pyrolysis of Waste Tires and Condensation Characteristics of Products in a Pilot Scale Screw-Propelled Reactor. *Fuel* **2023**, *353*, 129225. [CrossRef]

16. Wang, J.; Ma, Y.; Li, S.; Yue, C. Catalytic Pyrolysis of Polystyrene in Different Reactors: Effects of Operating Conditions on Distribution and Composition of Products. *J. Anal. Appl. Pyrolysis* **2024**, *177*, 106366. [[CrossRef](#)]
17. Wang, M.; Jia, T.; Song, X.; Yin, L.; Chen, D.; Qian, K. CFD–DEM Simulation of Heat Transfer and Reaction Characteristics of Pyrolysis Process of MSW Heated by High-Temperature Flue Gas. *Processes* **2024**, *12*, 390. [[CrossRef](#)]
18. Li, M.; Wang, L.; Luo, C.; Wu, H. A New Improved Fractional Tikhonov Regularization Method for Moving Force Identification. *Structures* **2024**, *60*, 105840. [[CrossRef](#)]
19. Ghasemi Monfared, Z.; Hellström, J.G.I.; Umeki, K. The Impact of Discrete Element Method Parameters on Realistic Representation of Spherical Particles in a Packed Bed. *Processes* **2024**, *12*, 183. [[CrossRef](#)]
20. Hilse, N.; Kriegeskorte, M.; Fischer, J.; Spatz, P.; Illana, E.; Schiemann, M.; Scherer, V. Discrete Element Simulations of Contact Heat Transfer on a Batch-Operated Single Floor of a Multiple Hearth Furnace. *Processes* **2023**, *11*, 3257. [[CrossRef](#)]
21. Liu, P.; Liu, J.; Gao, S.; Wang, Y.; Zheng, H.; Zhen, M.; Zhao, F.; Liu, Z.; Ou, C.; Zhuang, R. Calibration of Sliding Friction Coefficient in DEM between Different Particles by Experiment. *Appl. Sci.* **2023**, *13*, 11883. [[CrossRef](#)]
22. Cleary, P.W.; Sinnott, M.D.; Morrison, R.D. Scale-Up Investigation of a Pilot and Industrial Scale Semi-Autogenous Mill Using a Particle Scale Model. *Minerals* **2023**, *13*, 1490. [[CrossRef](#)]
23. Chen, J.; Ge, M.; Li, L.; Zheng, G. Material Transport and Flow Pattern Characteristics of Gas–Liquid–Solid Mixed Flows. *Processes* **2023**, *11*, 2254. [[CrossRef](#)]
24. Proch, F.; Bauerbach, K.; Grammenoudis, P. Development of an Up-Scalable Rotary Kiln Design for the Pyrolysis of Waste Tyres. *Chem. Eng. Sci.* **2021**, *238*, 116573. [[CrossRef](#)]
25. Hu, E.; Tian, Y.; Yang, Y.; Dai, C.; Li, M.; Li, C.; Shao, S. Pyrolysis Behaviors of Corn Stover in New Two-Stage Rotary Kiln with Baffle. *J. Anal. Appl. Pyrolysis* **2022**, *161*, 105398. [[CrossRef](#)]
26. Luo, H. Research on Material Flow Characteristics during Batch Compression Molding of Multi cavity Parallel Bottle Caps. Master's Thesis, South China University of Technology, Guangzhou, China, 2018.
27. Liu, P.; Ma, L.; Zeng, D.; Xiao, R. Study on material motion and mixing characteristics in a double helix reactor based on EDEM. *J. Sol. Energy* **2022**, *43*, 343–349. [[CrossRef](#)]
28. Xie, Q.; Chen, Z.; Hou, Q.; Yu, A.B.; Yang, R. DEM Investigation of Heat Transfer in a Drum Mixer with Lifters. *Powder Technol.* **2017**, *314*, 175–181. [[CrossRef](#)]
29. Kwapinska, M.; Saage, G.; Tsotsas, E. Mixing of Particles in Rotary Drums: A Comparison of Discrete Element Simulations with Experimental Results and Penetration Models for Thermal Processes. *Powder Technol.* **2006**, *161*, 69–78. [[CrossRef](#)]
30. Navarro, M.V.; Martínez, J.D.; Murillo, R.; García, T.; López, J.M.; Callén, M.S.; Mastral, A.M. Application of a Particle Model to Pyrolysis. Comparison of Different Feedstock: Plastic, Tyre, Coal and Biomass. *Fuel Process. Technol.* **2012**, *103*, 1–8. [[CrossRef](#)]
31. Zheng, H.; Wang, B.; Liu, R.; Zeng, D.; Xiao, R. Modelling of Large-Particle-Motion–Heat-Transfer Coupling Characteristics in Rotary Kiln Based on Discrete Element Method. *Int. J. Chem. React. Eng.* **2020**, *18*, 20200011. [[CrossRef](#)]
32. Deng, F. The effect of Wang Li tire particle size on pyrolysis products. *Appl. Chem.* **2019**, *48*, 1382–1384. [[CrossRef](#)]
33. Zhang, Z.; Liu, Y.; Zhao, X. Heat transfer characteristics of loose materials in the cross-section of Lei Xianming external heating rotary kiln. *J. Cent. South Univ. (Nat. Sci. Ed.)* **2018**, *49*, 2178–2183.
34. Han, W.; Jiang, C.; Wang, J.; Chen, H. Enhancement of Heat Transfer during Rubber Pyrolysis Process. *J. Clean. Prod.* **2022**, *348*, 131363. [[CrossRef](#)]
35. Fu, Y.; Wang, B.; Zheng, H.; Zeng, D.; Xiao, R. Simulation of Heat Transfer Characteristics of Tire Particles in Rotary Kiln Reactor. *Int. J. Chem. React. Eng.* **2021**, *19*, 1337–1349. [[CrossRef](#)]
36. Ramírez-Aragón, C.; Alba-Elías, F.; González-Marcos, A.; Ordieres-Meré, J. Segregation in the Tank of a Rotary Tablet Press Machine Using Experimental and Discrete Element Methods. *Powder Technol.* **2018**, *328*, 452–469. [[CrossRef](#)]

Disclaimer/Publisher's Note: The statements, opinions and data contained in all publications are solely those of the individual author(s) and contributor(s) and not of MDPI and/or the editor(s). MDPI and/or the editor(s) disclaim responsibility for any injury to people or property resulting from any ideas, methods, instructions or products referred to in the content.